*Acta Biologica Hungarica 59 (4), pp. 439–451 (2008)*
*DOI: 10.1556/ABiol.59.2008.4.5*

# MODELING AND BIOCHEMICAL ANALYSIS OF THE ACTIVITY OF ANTIBIOFILM AGENT DISPERSIN B

J. E. KERRIGAN,[1] C. RAGUNATH,[2] LILI KANDRA,[3]* GYÖNGYI GYÉMÁNT,[3] A. LIPTÁK,[3,4] L. JÁNOSSY,[3] J. B. KAPLAN[2] and N. RAMASUBBU[2]*

[1] Academic Systems and Technologies
[2] Department of Oral Biology, University of Medicine and Dentistry of New Jersey, 185 South Orange Ave, Newark NJ 07103
[3] Department of Biochemistry, Faculty of Sciences, University of Debrecen, P.O. Box 55, H-4010 Debrecen, Hungary
[4] Research Group for Carbohydrates of the Hungarian Academy of Sciences, University of Debrecen, P.O. Box 94, H-4010 Debrecen, Hungary

(Received: August 6, 2007; accepted: September 17, 2007)

Bacteria in a biofilm are enmeshed in a self-synthesized extracellular polysaccharide matrix (PGA), which is a linear polymer of β(1,6)-linked N-acetylglucosamine (GlcNAc) residues. Dispersin B (DspB), a soluble glycoside hydrolase produced by the periodontal pathogen *Actinobacillus actinomycetemcomitans* degrades PGA. The enzyme DspB is an α/β TIM-barrel protein and belongs to family 20 glycosyl hydrolases members. The enzyme activity of DspB with regard to its substrate specificity towards β(1,6)-linked GlcNAc polymers and its endo/exo character was investigated through ligand docking and the hydrolysis of synthetic oligosaccharides. Ligand docking analysis suggested that β(1,6)-linked GlcNAc oligosaccharide bound to the active site better that β(1,4)-linked GlcNAc oligosaccharide. Our combined results indicate that DspB is an exo-acting enzyme that hydrolyzes β(1,6)-linked N-acetylglucosamine oligomers.

*Keywords:* Biofilm – molecular modeling – Dispersin B – hydrolysis – HPLC – exo-acting

## INTRODUCTION

Sessile growth of bacteria on an abiotic surface, generally referred to as a biofilm, has been of immense interest due to the recent recognition of its role in the protection of bacteria and increase in the resistance to antimicrobial therapies. Two properties, adherence of bacterial cells to a surface and aggregation to each other, are critical for biofilm formation. *Actinobacillus actinomycetemcomitans* (Aa) is a Gram-negative coccobacillus that causes infections in humans, most notably localized aggressive periodontitis [22, 27]. *In vitro* studies have shown: 1. the tenacious adherence and attachment of planktonic cells to a surface [6] 2. the growth and develop-

*Corresponding authors; e-mail: kandra@puma.unideb.hu, ramasun1@umdnj.edu

ment of Aa into highly differentiated biofilm colonies [11] and 3. the detachment and dispersal of planktonic cells from the biofilm [11]. A soluble β-N-acetylglucosaminidase (Dispersin B abbreviated as DspB; EC 3.2.1.52; [11] mediates) the attachment and detachment properties of Aa to its biofilm. Interestingly, DspB exhibits biofilm detachment activity not only for Aa but also for biofilms produced by several bacterial species including Gram-positive species *(S. epidermidis)* and Gram-negative species (*A. pleuropneumoniae; E. coli; Yersinia pestis* and *Pseudomonas fluorescens* [8, 12]). The efficiency exhibited by DspB in preventing the biofilm formation of Aa and other bacterial species on abiotic surfaces creates a unique opportunity to develop this enzyme as an antibiofilm agent for the rapid removal of biofilms.

The enzyme DspB belongs to the family 20 glycosyl hydrolase members of which remove the terminal N-acetylglucosamine (GlcNAc) moiety from the non-reducing end. The enzyme activity of DspB has been investigated using polymeric β(1,6)-N-acetyl-D-glucosamine (PGA) from *E. coli* which showed that the reaction products included GlcNAc and other unassigned GlcNAc oligomers [8]. Although this study suggested that DspB was an endolytic enzyme, there is paucity of information on the endo/exo character of DspB towards the hydrolysis of PGA especially since the family 20 hydrolases are generally classified as exo-acting enzymes. While some members of family 20 hydrolases exhibit broad substrate specificity, DspB appears to be specific to PGA. In order to clarify the nature of the enzymatic activity of DspB with regards to its substrate specificity, we undertook molecular modeling studies of the docking between an oligosaccharide (both β(1,4)- and β(1,6)-linkages) and the enzyme using the crystal structure of DspB (PDB Code 1YHT) [21]. To further investigate whether DspB is an endo- or exo-acting enzyme, we used oligosaccharides containing β(1,6)-GlcNAc as substrates and analyzed the reaction products using HPLC. Our results clearly show that DspB is an exo-acting enzyme with the binding pocket especially suited for β(1,6) linkages.

## MATERIALS AND METHODS

### *Docking methods*

Since the enzyme DspB used in the present study was a His.Tag protein, and the crystal of this expressed protein did not reveal residues at the N- and C-termini, these missing residues and disordered residues (residues 187–191) in the source PDB file (1YHT) were repaired using the *profix* program (Jackal software package) [26]. The β(1,4)- and β(1,6)-linked N-acetyl-glucosamine saccharides (NAG) were built using the Leap program in Amber 8 [3], and their geometry optimized using the glycam04 force field [13]. The saccharide and protein input files were prepared using Sybyl (Tripos, Inc.). Gasteiger charges were used on the saccharides and Amber99 charges were used on the protein [25]. We performed dockings using UCSF DOCK program (v 5.2) [14]. The bump and energy grids were set up such that the entire active site

was covered. The active site cleft was assumed to be the site where glycerol and acetate ion were bound in the native enzyme (PDB Code 1YHT).

## *Molecular dynamics and binding free energy estimates*

The docked model containing both the enzyme and the substrate were subjected to molecular dynamics. All dynamics computations were performed on a SunFire 6900 multiple CPU server. All explicit solvation calculations were performed using the GROMACS 3.2 software package [15]. The simulation was performed using the modified GROMOS87 force field [24] with apolar hydrogen atoms treated as united atoms, and solvated using the SPC rigid water model [2] in a shell of water molecules. The flexible SPC water model [5] was used in preliminary steepest descents minimization only. GROMOS87 charges were used on the entire system. The saccharides were parameterized using the PRODRG program [23]. All bonds were constrained using the LINCS algorithm [7]. The SETTLE algorithm was used to constrain the bonds in the SPC rigid water model [19]. Smooth decay of electrostatic and van der Waals interactions were modeled using a shift function. The solvated system was pre-minimized using a steepest descent approach to a gradient of 1000 to remove bad van der Waals contacts. The water molecules in the system were equilibrated using 20 ps of NPT molecular dynamics simulation using a 2 fs time step at 300 °K using the Berendsen thermostat while keeping the protein-NAG complex atom positions restrained [2]. The resulting structure was used for the overall molecular dynamics simulation of the entire solvated system using the NVT ensemble at 300 °K. The dynamics runs were performed using a 2 fs time step snapshot every 1 ps, at 300 °K. The structure averages were taken from the 200 to 500 ps range of each simulation. Each average structure was refined using steepest descents energy minimization to a gradient of 1000 followed by L-BFGS energy minimization to a gradient of 50. Molecular dynamics simulations on the individual saccharides were run using the same parameters as for the complexes with the exception that the saccharide runs were of 250 ps duration with no counter ions as the saccharides are neutral. The dynamics data generated above were used to compute estimates of binding free energy using the linear interaction energy (LIE) method [1]. Energy data from the region of equilibrium (200 to 500 ps) in the complex were used for the saccharide/protein interaction energy averages. The entire ensemble averages were used for the saccharide/water energy component averages.

## *Hydrolysis of GlcNAc oligosaccharides*

The enzyme DspB was expressed and purified using the plasmid pRC3 that carried the *dspB* gene encoding amino acids 21 to 381 fused directly to a hexahistidine metal-binding C-terminal tail located downstream from an IPTG-inducible *tac* promoter as previously described [21]. The β(1,6)-linked oligosaccharides, 4-methoxy-

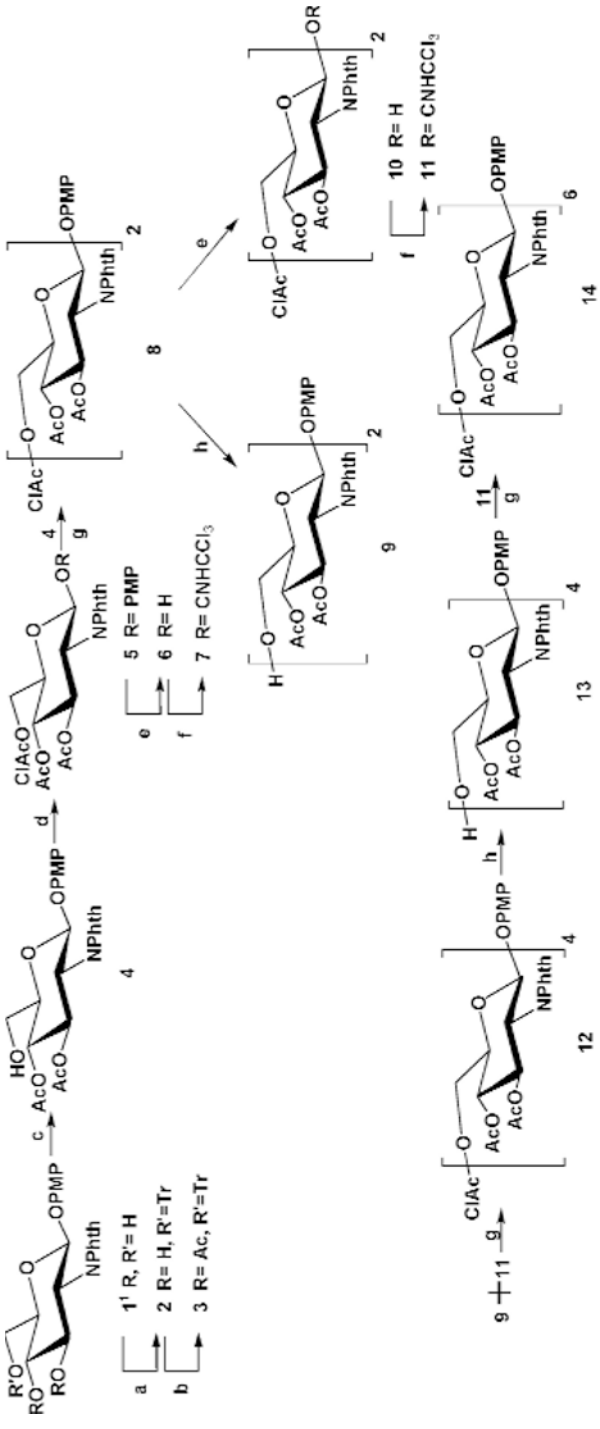

*Fig. 1.* Reagents and conditions: (a) triphenylmethyl chloride, DMAP, Py, rt, 48 h; (b) $Ac_2O$, Py, rt, 24 h; (c) acetic acid-$H_2O$, 55 °C, 2 h; (d) chloroacetyl chloride, Py, DCM, –10 °C → rt, 0.5 h; (e) CAN, toluene-DCM-$H_2O$, 0 °C, 1 h; (f) trichloroacetonitrile, DBU, DCM, rt, 24 h; (g) $BF_3.Et_2O$, DCM, 0 °C, 1 h; (h) thiourea, DCM-MeOH, 50 °C, 2 h; (k) 1. 72% hydrazine in $H_2O$, 85 °C, 2 h; 2. $Ac_2O$, Py, rt, 24 h; 3. NaOMe, MeOH, rt, 24 h

phenyl 2-deoxy-2-N-acetyl-β-D-glucosamine (PMP-GlcNAc) glycosides (DP 1, 2, 4 and 6) were chemically synthesised using standard procedures (Fig. 1). For the preparation of *p*-metoxyphenyl oligomers N-phthaloyl participating protecting group was used at position 2, which ensures the formation of 1-2 trans interglycosidic bond. Primary hydroxyl group was protected by chloroacetyl temporary protecting group. Donor compounds were obtained as trichloroacetimidate. 2 + 2 and 2 + 4 block syntheses were performed for the preparation of longer oligosaccharide substrates. Structure of compounds was confirmed by NMR and MALDI TOF MS measurements.

Hydrolytic reactions were carried out using β(1,6)-linked GlcNAc oligosaccharides and the reaction products were analyzed by HPLC to investigate the substrate specificity of DspB. Incubations of the various oligosaccharides with varying degree of polymerization (DP = 2, 4 or 6) in 50 mM phosphate buffer (pH 5.9) containing 100 mM NaCl were carried out at 37 °C for 1, 3, 5 and 20 h. The reactions were initiated by the addition of 7.2 μM of enzyme. For HPLC analysis, 20 μL of the reaction mixture was injected into the chromatographic column at times indicated above. Reaction products were separated on a reversed phase column (Chromolith, RP18a, 100 × 4.6 mm) with acetonitrile : water (8 : 92) as the mobile phase at a flow rate of 1 ml/min at 25 °C using a Hewlett-Packard 1090 Series II liquid chromatograph equipped with diode array detector and automatic sampler. Effluent was monitored for the products containing *p*-methoxyphenyl group at 280 nm and the products of the hydrolysis were identified by using relevant standards and analyzed using ChemStation software. The quality of the acetonitrile used was of HPLC gradient grade. Purified water was obtained from a laboratory purification system equipped with both ion exchange and carbon filters (Millipore, Bedford, MA, USA).

## RESULTS AND DISCUSSION

### *Docking of β-linked oligomers*

While most of the hitherto reported hexosaminidase enzymes cleave substrates with β(1,4)-linkage, the substrate for DspB appears to be a polymer consisting of β(1,6)-linked N-acetylglucosamine residues [8, 12]. In order to further delineate on the substrate specificity of DspB towards β(1,6)-linkages, we undertook the docking studies using both linkages to define the structural determinants at the active site of DspB. We modeled a trisaccharide and a larger tetrasaccharide containing either β(1,4) or β(1,6)-linkages to cover as many subsites, if any, as possible in DspB. The active site of DspB has been identified earlier from its crystal structure [21]. Using this structure (PDB Code 1YHT), the bump and energy grids for docking were generated to encompass the active site. The bump grids were used for screening and filtering out atomic overlaps (bad van der Waals contacts) between ligand and receptor. The UCSF-DOCK program scores the energy function as a sum of electrostatic ($E_{elec}$) and van der Waals ($E_{vdw}$) energies and uses the AMBER 99 parameters [3]. The energy

*Table 1*
Energy score results from UCSF DOCK. Energies are given in kcal/mol

| Complex | $E_{vdw}$ | $E_{elec}$ | $E_{score}$ | $E_{rel}$ |
|---|---|---|---|---|
| β 1-4triNAG-DspB | –50.68 | –10.15 | –60.83 | 0.0 |
| β 1-6triNAG-DspB | –54.63 | –7.99 | –62.62 | –1.8 |
| β 1-4tetraNAG-DspB | –56.44 | –8.83 | –65.26 | –4.4 |
| β 1-6tetraNAG-DspB | –67.04 | –5.77 | –72.81 | –11.9 |

$E_{rel} = E_{score}$ (complex) – $E_{score}$ (β 1-4triNAG-DspB)

*Table 2*
LIE results

| Complex | $\Delta G_{bind}$ (kcal/mol) | $\Delta\Delta G_{bind}$ (kcal/mol) |
|---|---|---|
| β 1-4 triNAG:DspB | –17.1 | 0.0 |
| β 1-6 triNAG:DspB | –22.5 | –5.4 |
| β 1-4 tetraNAG:DspB | –12.4 | +4.7 |
| β 1-6 tetraNAG:DspB | –28.3 | –11.2 |

$\Delta\Delta G_{bind} = \Delta G_{bind}$ (complex) – $\Delta G_{bind}$ (β 1-4 triNAG:DspB)
$\Delta G_{bind} = -RT\ln K$ (for comparison with experimental data)

scores for the average structures of the oligomers of β(1,4)-NAG and β(1,6)-NAG (DP = 3 and 4) docked to the enzyme is given in Table 1. For comparison purposes, the relative energies were normalized using the energy value for β(1,4)-NAG trimer complexed to the enzyme. The complexes formed by the β(1,6)-linked NAG oligomers scored better than the β(1,4)-linked oligomers. The docking study revealed that the β(1-4)-linked saccharides bind in a different but less efficient orientation relative to the β(1-6)-linked saccharides (Fig. 2). This is not surprising from the standpoint that the β(1-4)-linked saccharides are more linear as compared to the β(1-6)-linked saccharides, which have some curvature to their chain structure and therefore are more compact. For the tetrasaccharides, the curvature of the β(1-6)-linked saccharide permits it to make additional contacts with the broader binding site of DspB leading to stronger binding. We also noted that hydrogen bonding alone did not explain the greater stability of the β(1-6)- *vs*. the β(1-4)-linked saccharide in both the tri- and tetrasaccharides. A greater contributor to the stability appears to be hydrophobic (van der Waals) interactions. The β(1-6)-linked saccharide fills the shape of the extended site much more than the β(1-4)-linked saccharide in both the tri- and tetrasaccharide models.

We also assessed the free energy estimates for the bound oligomer compared to the unbound oligomers after a molecular dynamics (MD) simulation using the DOCK-generated bound conformation. The MD simulations revealed that β(1,4)-NAG tetramer adopted a single conformation while the β(1,6)-NAG tetramer adopts two

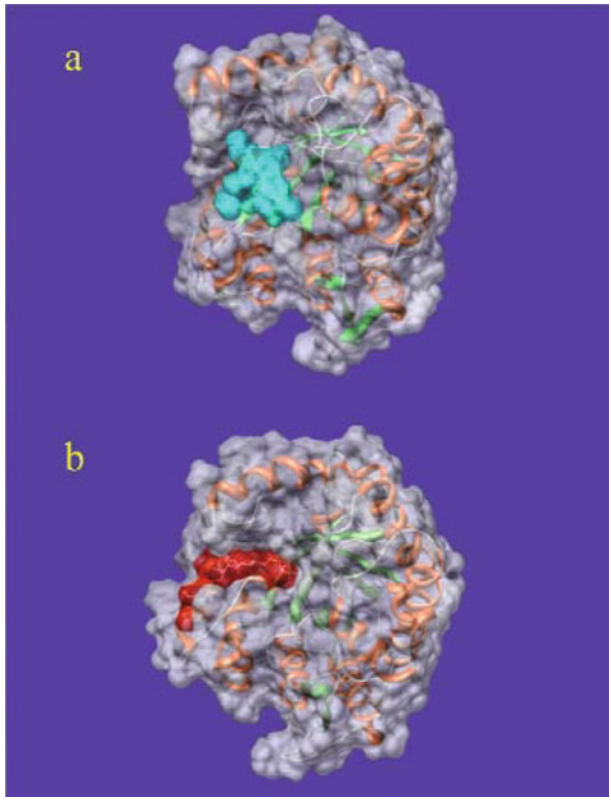


*Fig. 2.* Docked β(1,4)-oligosaccharides (a) and β(1,6)-oligosaccharides (b) in the active site of DspB. Note that the β(1,4)-saccharide is loosely fit and not completely inside the binding pocket. In contrast, β(1,6)-saccharide is snugly fit into the active site in a tight manner

conformations albeit the second conformation is of much higher energy. When MD simulations were carried out in the presence of the enzyme DspB, the β(1,6)-linked oligomers (both tri- and tetra-) consistently bound to DspB better as shown by the Linear Interaction Energies (Table 2). These results are consistent with earlier observations that DspB does not cleave β(1,4)-linkages as in chitin and substantiates an earlier report that the substrate for DspB is the PGA polymer containing β(1,6)-linked GlcNAc [8, 10].

## *Analysis of the active site of DspB*

Our study provides some answers to the question of β(1,6)- linkage specificity exhibited by DspB compared to the bacterial β-hexosaminidases exhibiting β(1,4) specificity as shown below. The lower average structure obtained from the molecular

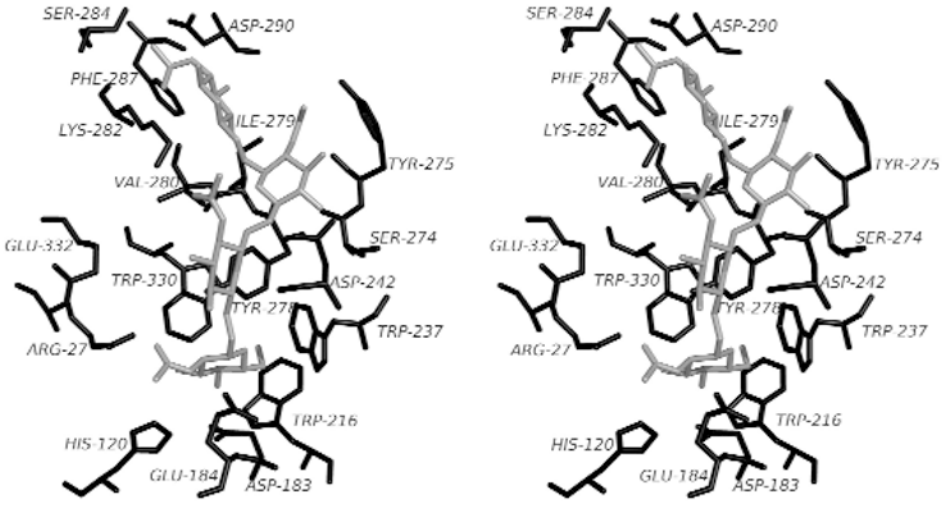


*Fig. 3.* Stereodiagram of the active site of the DspB : β(1,6)-linked GlcNAc tetrasaccharide. Protein atoms are shown in black while those of the tetrasaccharide are shown in grey. Note the presence of four subsites with subsite –1 at the bottom of the figure and subsite +3 at the top. Subsite –1 contains Asp183, Glu184, and Arg27 in close proximity (< 3.5 A), which interact with a GlcNAc. Several other residues including the aromatic residues Trp216, Trp237, Tyr278, and Trp330 provide stacking interactions to the bound saccharides. All these residues are well conserved in the family 20 hexosaminidases. Notable absence is a residue equivalent to Trp408 of bacterial hexosaminidase (PDB Code 1HP5)

dynamics simulation analysis was used to analyze the interactions between the DspB enzyme and the docked substrates. The binding of β(1,4)-linked tetramer appears to be shifted and out of the binding pocket whereas the β(1,6)-linked tetrasaccharide fits snugly in the active site pocket (Fig. 1). As a result, DspB: β(1,4)-tetrasaccharide complex does not show the characteristic binding of a GlcNAc moiety into the pocket provided by the three conserved aromatic residues. On the other hand, the active

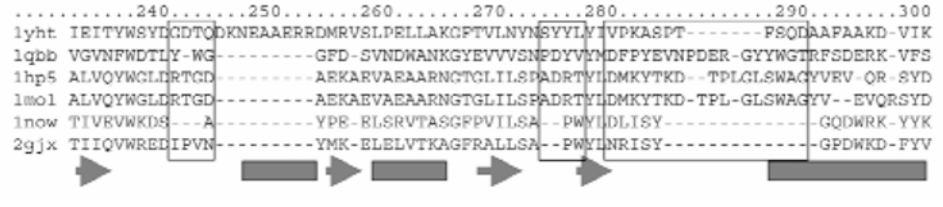


*Fig. 4.* Structure-based sequence alignment of β-hexosaminidases (PDB codes are shown on the left). Residues forming the subsites +2, +3 at the active site are present in a less conserved region (boxed segment). Note that such variability in the sequence might account for the substrate specificity exhibited by DspB towards β(1,6)-linkages. Arrows represent β-strands and rectangles are α-helices corresponding to the secondary structures derived from the DspB crystal structure 1YHT [20]

site architecture of the DspB-tetrasaccharide model has several salient features that are characteristic of hexosaminidases. These include the presence of a Glu residue in the vicinity of the glycosidic linkage (Glu184) and three Trp residues surrounding a bound terminal saccharide [17, 18]. The DspB: β(1,6)-tetrasaccharide complex shows that several residues, Arg27, His120, Asp183, Glu184, Trp216, Trp237, Asp242, Ser274, Tyr275, Tyr278, Ile279, Val280, Lys282, Ser284, Phe287, Asp290, and Trp330 (Fig. 3), form the active site forming at least four subsites named –1, +1, +2 and +3 [4]. Residues Arg27, His120, Asp183, Glu184, Trp216, Trp237, Tyr278, and Trp330 form subsite –1, generally occupied by a terminal GlcNAc at the non-reducing end. An invariant residue in most hexosaminidases, His120, is also in the vicinity of subsite –1. Although subsite –1 is highly conserved in the family 20 enzymes, there are significant differences in residues forming the remainder of the binding sites (Fig. 4). For example, in human as well as in bacterial hexosaminidases, the residues Trp685 and Trp408, respectively, interact with the +1 subsite moiety via hydrophobic stacking interactions. The absence of an equivalent Trp residue in DspB is consistent with the conformational difference due to a curved β(1,6)-linked oligomer.

Different enzymes in a given family can have different specificities as has been noted before in the α-amylase family [16]. In these enzymes, activity involves binding a glucose residue of the substrate at subsite –1, while the amino acid residues constituting the substrate binding at subsites +1 and +2 varies with the specificity of the enzyme whether α-1,4 or α-1,6. This is clearly seen in DspB as well. While most of the conserved residues appear at the subsite –1, largest differences occur at subsites +1, +2 and +3 (Fig. 4). The sequence of DspB has least similarity with other hexosaminidases after position 278 (Tyr). In fact, many hexosaminidases have gaps in this region suggesting that there is flexibility in this region. When enzymes belonging to the same family act on different types of linkages (GH-20; β-1,4 *vs*. β-1,6), some flexibility at the active site is expected. Otherwise, a 4-linked N-acetylglucosamine and a 6-linked N-acetylglucosamine cannot fit in an identical way into an active site. It is tempting to suggest that hydrolysis in DspB occurs via a different mechanism since the binding mode in DspB is different at subsite –1 compared to the β-hexosaminidases that cleave β(1,4)-linkages. Mutational studies involving the identified active site residues are in progress to analyze the mechanistic aspects of the hydrolysis reaction.

## *Hydrolysis of GlcNAc oligosaccharides*

The endo/exo-active nature of DspB was analyzed using HPLC on GlcNAc oligosaccharides (Fig. 5). We would like to emphasize the production of oligosaccharides with DP of $n-1$ (where the DP of the substrate is $n$) in HPLC analysis of product distributions of three β(1,6)-linked GlcNAc oligosaccharides. The $n-1$ products of the first cleavage are further hydrolyzed to generate oligosaccharides with a DP of $n-2$,

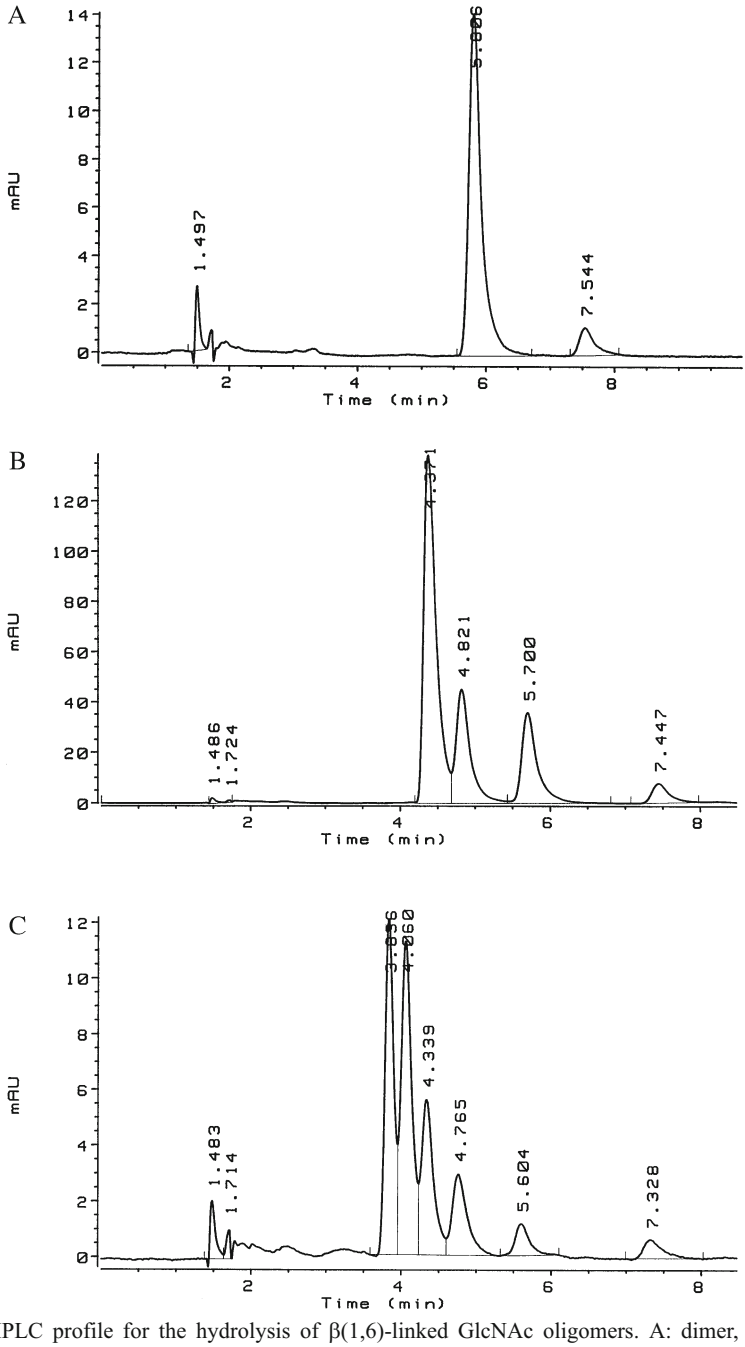


*Fig. 5.* HPLC profile for the hydrolysis of β(1,6)-linked GlcNAc oligomers. A: dimer, B: tetramer, C: hexamer. Retention order is reversed on C18 phase, first eluted peaks are the substrates followed by the shorter hydrolysis products

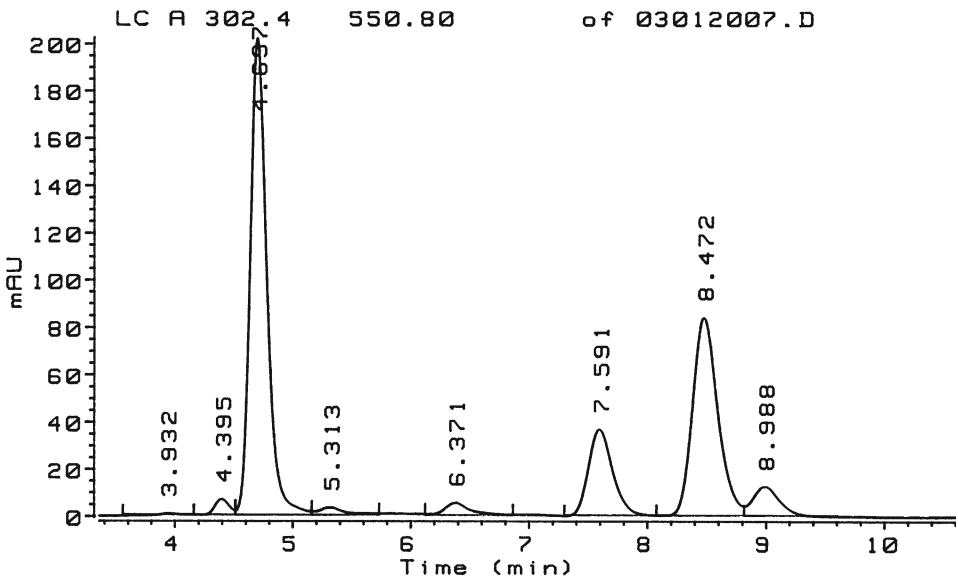


*Fig. 6.* RP-HPLC profile for the hydrolysis of a maltohexamer glycoside catalysed by Y151M mutant of HSA. First peak is the substrate followed by products DP 5-1

$n-3$ and so on. For example, the GlcNAc dimer generates PMP-GlcNAc with a very low intensity of the monomer due to further cleavage of the aglycone *p*-methoxyphenol. The GlcNAc tetramer produced trimer (48.5%), dimer (41.4%) and monomer (10.1%) compounds. Similarly, the hexasaccharide resulted in the formation of pentamer (45.7%), tetramer (25.6%), trimer (17%), dimer (6%) and monomer (5.7%) products. The HPLC cleavage pattern is consistent with an exo-acting enzyme whose substrates are labeled at the reducing end. An endo-acting enzyme such as human salivary α-amylase (HSA) produces more di- and trisaccharides than either penta or tetra when the substrate is a hexasaccharide. An example can be seen in Figure 6 where CNP-$G_6$ is hydrolyzed by Y151M mutant of HSA [9]. In conclusion, we have shown through molecular modeling analysis and hydrolysis of oligosaccharide substrates that the substrate for DspB is a β(1,6)-linked GlcNAc polymer. We also show that DspB is an *exo* enzyme acting on short oligosaccharides and capable of releasing terminal N-acetylglucosamine residues from the non-reducing end.

ACKNOWLEDGEMENTS

This project was supported by the USPHS Grants DE16291 (N.R.), DE15124 (J.B.K.) and OTKA Grants T047075 (L.K.), AT48798 (A.L.). The authors thank the Scientific Server Resource managed by Academic Systems Group in IST, UMDNJ for computer time.

REFERENCES


1. Aqvist, J., Marelius, J. (2001) The linear interaction energy method for predicting ligand binding free energies. *Comb. Chem. High Throughput Screen 4,* 613–626.
2. Berendsen, H. J., Postma, J. P., M. Van Gunsteren, W. F., Hermans, J. (1981) Interaction models for water in relation to protein hydration. In: Reidel, D. (ed.) *Intermolecular Forces.* Dordrecht, The Netherlands, pp. 331–342.
3. Case, D. A., Chetham, I., Darden, T., Gohlke, H., Luo, R., Merz, K. M., Onufriev, A., Simmerling, C., Wang, B., Woods, R. (2005) The amber biomolecular simulation programs. *J. Comput. Chem. 26*, 1668–1688.
4. Davies, G. J., Wilson, K. S., Henrissat, B. (1997) Nomenclature for sugar-binding subsites in glycosyl hydrolases. *Biochem. J. 321* (Pt 2) 557–559.
5. Ferguson, D. (1995) Parameterization and evaluation of a flexible water model. *J. Comput. Chem. 16,* 501–511.
6. Fine, D. H., Furgang, D., Kaplan, J., Charlesworth, J., Figurski, D. H. (1999) Tenacious adhesion of *Actinobacillus actinomycetemcomitans* strain CU1000 to salivary-coated hydroxyapatite. *Arch. Oral. Biol. 44,* 1063–1076.
7. Hess, B., Bekker, H., Berendsen, H. J. C., Fraaije, J. G. E. M (1997) LINCS: A linear constraint solver for molecular simulations. *J. Comp. Chem. 18,* 1463–1472.
8. Itoh, Y., Wang, X., Hinnebusch, B. J., Preston, J. F. 3rd, Romeo, T. (2005) Depolymerization of beta-1,6-N-acetyl-D-glucosamine disrupts the integrity of diverse bacterial biofilms. *J. Bacteriol. 187,* 382–387.
9. Kandra, L., Gyémánt, G., Remenyik, J., Ragunath, C., Ramasubbu, N. (2003) Subsite mapping of human salivary α-amylase and the mutant Y151M. *FEBS Lett. 544*, 194–198.
10. Kaplan, J. B., Meyenhofer, M. F., Fine, D. H. (2003) Biofilm growth and detachment of *Actinobacillus actinomycetemcomitans. J. Bacteriol. 185*, 1399–1404.
11. Kaplan, J. B., Ragunath, C., Ramasubbu, N., Fine, D. H. (2003) Detachment of *Actinobacillus actinomycetemcomitans* biofilm cells by an endogenous beta-hexosaminidase activity. *J. Bacteriol. 185*, 4693–4698.
12. Kaplan, J. B., Ragunath, C., Velliyagounder, K., Fine, D. H., Ramasubbu, N. (2004) Enzymatic detachment of *Staphylococcus epidermidis* biofilms. *Antimicrob. Agents Chemother. 48,* 2633–2636.
13. Kirschner, K. N., Woods, R. J. (2001) Solvent interactions determine carbohydrate conformation. *Proc. Natl. Acad. Sci. USA 98,* 10541–10545.
14. Kuntz, I. D., Meng, E. C., Shoichet, B. K. (1994) Structure-based molecular design. *Acc. Chem. Res. 27,* 117–123.
15. Lindahl, E., Hess, B., van der Spoel, D. (2001) GROMACS 3.0: a package for molecular simulation and trajectory analysis. *J. Mol. Model. 7*, 306–317.
16. MacGregor, E. A., Janecek, S., Svensson, B. (2001) Relationship of sequence and structure to specificity in the alpha-amylase family of enzymes. *Biochim. Biophys. Acta 1546,* 1–20.
17. Maier, T., Strater, N., Schuette, C. G., Klingenstein, R., Sandhoff, K., Saenger, W. (2003) The X-ray crystal structure of human beta-hexosaminidase B provides new insights into Sandhoff disease. *J. Mol. Biol. 328*, 669–681.
18. Mark, B. L., Vocadlo, D. J., Knapp, S., Triggs-Raine, B. L., Withers, S. G., James, M. N. (2001) Crystallographic evidence for substrate-assisted catalysis in a bacterial beta-hexosaminidase. *J. Biol. Chem. 276,* 10330–10337.
19. Miyamoto, S., Kollman, P. A. (1992) SETTLE: An analytical version of the SHAKE and RATTLE algorithms for rigid water models. *J. Comp. Chem. 13*, 952–962.
20. Ramasubbu, N., Ragunath, C., Mishra, P. J. (2003) Probing the role of a mobile loop in substrate binding and enzyme activity of human salivary amylase. *J. Mol. Biol. 325,* 1061–1076.
21. Ramasubbu, N., Thomas, L. M., Ragunath, C., Kaplan, J. B. (2005) Structural analysis of dispersin B, a biofilm-releasing glycoside hydrolase from the periodontopathogen *Actinobacillus actinomycetemcomitans*. *J. Mol. Biol. 349*, 475–486.

22. Slots, J., Genco, R. J. (1984) Black-pigmented Bacteroides species, Capnocytophaga species, and *Actinobacillus actinomycetemcomitans* in human periodontal disease: virulence factors in colonization, survival, and tissue destruction. *J. Dent. Res. 63*, 412–421.
23. Van Aalten, D. M., Bywater, R., Findlay, J. B., Hendlich, M., Hooft, R. W., Vriend, G. (1996) PRODRG, a program for generating molecular topologies and unique molecular descriptors from coordinates of small molecules. *J. Comput. Aided Mol. Des. 10*, 255–262.
24. Van Gunsteren, W. F., Berendsen H. J. (1987) *Gromos-87 Manual.* Biomos BV:AG Groningen, The Netherlands.
25. Wang, J., Cieplak, P., Kollman, P. A. (2000) How well does a restrained electrostatic potential (RESP) model perform in calculating conformational energies of organic and biological molecules? *J. Comput. Chem. 21,* 1049–1074.
26. Xiang, J. Z. (2002) *A Protein Structure Modeling Package.* Columbia University, New York, NY.
27. Zambon, J. J. (1985) *Actinobacillus actinomycetemcomitans* in human periodontal disease. *J. Clin. Periodontol. 12,* 1–20.